

## SUPPORTING INFORMATION

### Monitoring structural changes in intrinsically disordered proteins with QCM-D: Application to the bacterial cell division protein ZipA

P. Mateos-Gil, A. Tsortos\*, M. Velez, E. Gizeli\*

#### Materials and Methods

##### 1. Chemicals

Analytical grade chemicals were purchased from Merck or Sigma. Lipids, 1,2-dioleoyl-sn-glycero-3-[(N-(5-amino-1-carboxypentyl)iminodiacetic acid)succinyl] (DGS-NTA ( $\text{Ni}^{2+}$ )) and L- $\alpha$ -phosphatidyl-choline from chicken egg (EPC) were purchased from Avanti Polar Lipids (Alabaster, AL, USA).

##### 2. Liposome preparation

Lyophilized lipids were dissolved in 1:1 chloroform:methanol solution, mixed in the desired amount (EPC:DGS-NTA, 9:1 molar ratio), dried under a stream of nitrogen and resuspended at 2 mg/ml total lipid concentration in Tris-HCl 10 mM, NaCl 200 mM, pH 7.5. The resulting multilamellar vesicle solution was extruded through polycarbonate membrane with 50-nm nominal pore diameter (LiposoFast, Avestin) leading to a stock solution of unilamellar vesicles and stored at 4 °C for five days maximum.

##### 3. Protein purification

The soluble constructs of ZipA (s1ZipA and s2ZipA) were produced by eliminating the hydrophobic N-terminal domain (a.a 1-25) and the hydrophobic N-terminal domain plus the intrinsic disordered domain (a.a 1-188) of the full length protein respectively, as described elsewhere<sup>1</sup>. Protein fractions were pooled and stored at -80 °C. The purity of s1ZipA and s2ZipA was > 95% according to SDS-PAGE.

##### 4. Quartz crystal microbalance with dissipation monitoring (QCM-D)

A QCM-D (Q-Sense E4, Sweden) capable of measuring changes in resonance frequency  $\Delta f$  and energy dissipation  $\Delta D$  was used. Measurements reported here were performed at operating frequency of 35 MHz (i.e., seventh overtone), with continuous flow rate of 50  $\mu\text{l}/\text{min}$  and fixed temperature of 25 °C. To ensure a clean and highly hydrophilic surface of crystal sensors,  $\text{SiO}_2$  coated sensors (Q-Sense QSX 303) were cleaned with Hellmanex 2%, dried under nitrogen, and treated for 2.5 min using a plasma cleaner (Harrick PDC-002, USA) at "HI" setting immediately prior to each experiment.

##### 5. Real-time acoustic detection of s1ZipA and s2ZipA binding onto supported lipid bilayer (SLB)

A continuous flow of Tris-HCl 10 mM, NaCl 200 mM, pH 7.5 was pumped through the QCM-D chamber and the acoustic signal was allowed to equilibrate prior to the first addition. A SLB was formed upon injection of 0.05 mg/ml vesicle solution using the same buffer with an additional 5 mM  $\text{NiCl}_2$ . After lipid bilayer formation, the working buffer was replaced by TMK500 (Tris-HCl 50 mM, KCl 500 mM, 5 mM  $\text{MgCl}_2$ , pH 7.5), protein solutions at different concentrations (0.1 to 1.2  $\mu\text{M}$  and 0.1 to 0.6  $\mu\text{M}$  for s1ZipA and s2ZipA respectively) were pumped through the chamber, and s1ZipA or s2ZipA binding to the bilayer was recorded. Subsequent buffer exchanges with different salt content (see Table 1) were performed to record in real time variations in the ratio of dissipation to frequency change ( $\Delta D/\Delta f$ ) as a function of ionic strength.

Table 1. Ionic buffer content.

	Tris-HCl	KCl	$\text{MgCl}_2$	pH
TMK500	50 mM	500 mM	5 mM	7.5
TK500	50 mM	500 mM	-	7.5
TK50	50 mM	50 mM	-	7.5
TK5	50 mM	5 mM	-	7.5
TK0	50 mM	-	-	7.5

## 6. Intrinsic viscosity measurement

For the measurement of viscosity and the subsequent calculation of the intrinsic viscosities, protein samples were prepared at various initial concentrations ( $\approx 0.2 - 4.0$  mg/ml) as determined with the Bradford method, in Tris buffer (50 mM Tris, pH 7.5) and the appropriate KCl content; these concentrations are in the dilute regime. An automated microviscometer (AMVn-Anton Paar) was used. All measurements were performed at a fixed angle of 30 deg, with a 0.9 mm diameter glass capillary and a volume of 150  $\mu$ l; the temperature was set at 25 °C. Calibration was performed according to the supplier's instructions; each measurement was repeated at least three times.

## 7. Calculation of hydrodynamic radius from $[\eta]$ and HYDROPRO software

The hydrodynamic radius  $R_h$  can be calculated directly from the  $[\eta]$  experimental data since it is known<sup>2</sup> that  $R_h \approx R_v$  (within less than 10%)<sup>3</sup> for many molecular shapes;  $R_v$  represents the equivalent-sphere viscosity radius and is given by

$$R_{viscous}^3 = \frac{3}{10\pi N_A} Mw[\eta] \quad \text{Eq. S1}$$

For the calculations with HYDROPRO of the hydrodynamic radius of the structures shown in Figure 1 (in the main text), the NMR atomic structure (1F7W.pdb) of s2ZipA was used<sup>4</sup>. The PyMOL Molecular Graphics System (Schrödinger, LLC) was used for protein drawing.

## SUPPLEMENTARY FIGURES

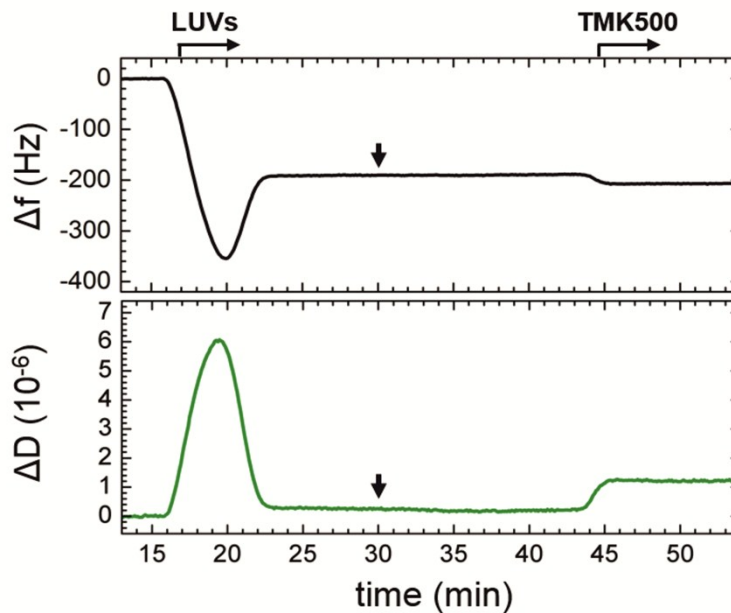


Figure S1. SLB formation followed by quartz crystal microbalance (QCM-D); the vertical arrow indicates buffer rinsing.

A SLB (Fig. S1) was formed upon addition of 0.05 mg/ml liposome solution (LUVs). The final frequency and dissipation changes (upper and lower panel respectively),  $\Delta f_7 = -200$  Hz (i.e., normalized change  $\Delta f_7/7 = -28$  Hz) and  $\Delta D_7 = 0.3 \times 10^{-6}$ , and the transient presence of a minimum frequency and a maximum dissipation confirmed the formation of a complete and homogeneous bilayer as described previously<sup>5</sup>. A small frequency and dissipation shift,  $\Delta f_7 = -20$  Hz and  $\Delta D_7 = 1.0 \times 10^{-6}$  was observed upon exchange between liposome adsorption buffer and high salt protein buffer (TMK500) owing to differences in buffer density and viscosity.

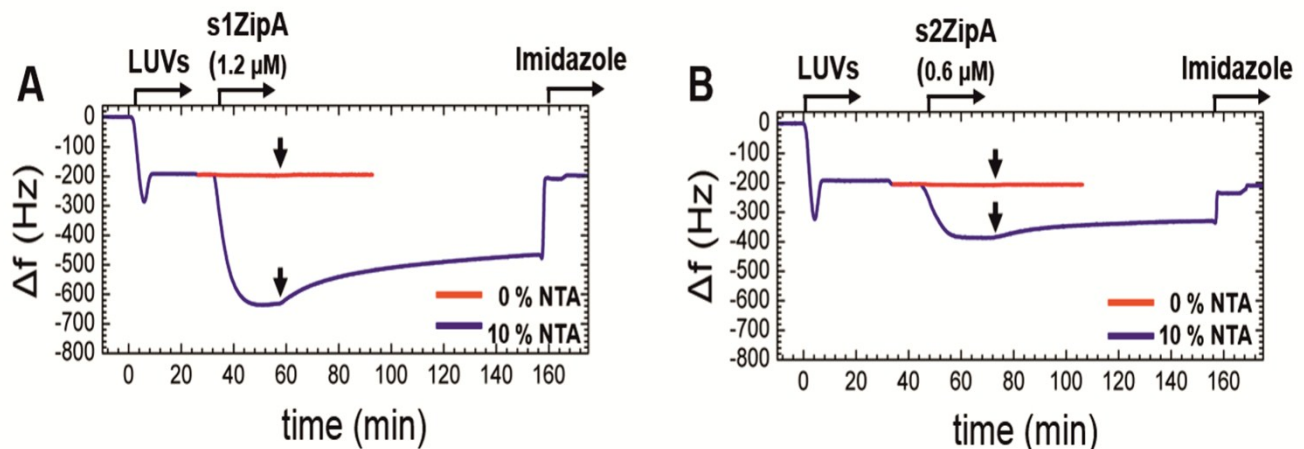


Figure S2. Binding specificity of His-tagged ZipA soluble constructs (s1ZipA, s2ZipA) to SLBs

Strong change in frequency was observed upon addition of His-tagged proteins indicating surface attachment (Fig. S2). Passing of s1ZipA 1.2  $\mu\text{M}$  (A) and s2ZipA 0.6  $\mu\text{M}$  (B) solutions over a lipid bilayer containing 10% NTA lipids was enough to saturate the surface in  $\approx 25$  minutes (blue line). Excess protein was washed off the surface after rinsing (vertical

arrow), leading to a non-stable base line. Exposure of equally concentrated s1ZipA and s2ZipA solutions to a bilayer lacking NTA lipids (red line) led to no frequency shift indicating the absence of surface attachment. In addition, complete elution of surface anchored proteins by imidazole (200 mM) was observed confirming the binding specificity of His-tagged ZipA soluble constructs to SLBs through the interaction between Histidine tags and NTA/ $\text{Ni}^{2+}$  chelating groups.

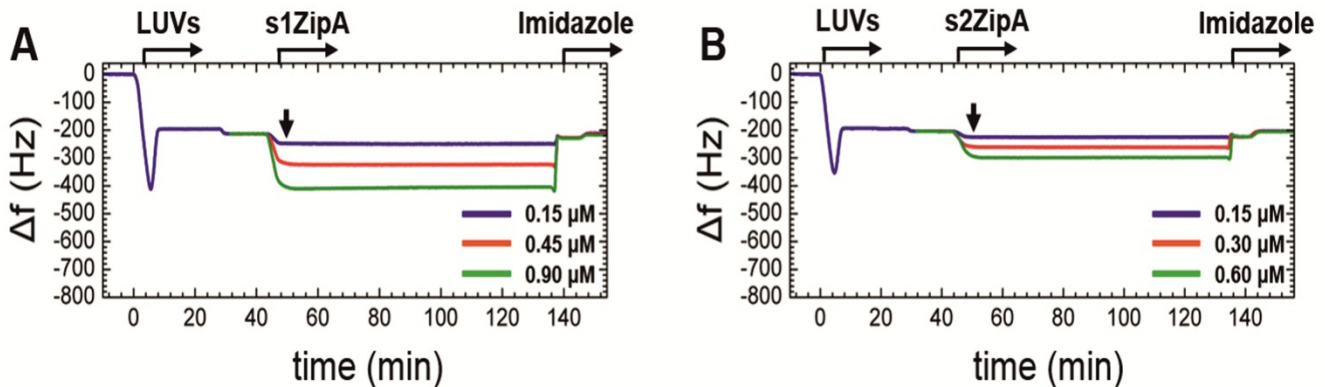


Figure S3. Binding stability of His-tagged ZipA soluble constructs (s1ZipA and s2ZipA) anchored onto SLBs

We identified the level of surface deposition where s1ZipA and s2ZipA remain stably anchored to the surface. Long incubation times at high protein concentrations led to high surface attachment but proteins washed off the surface, as indicated by a non stable baseline, after a buffer rinse (Fig. S2). In contrast, smaller frequency changes were observed upon injections of less concentrated protein solutions for  $\approx 3$  minutes. Figure S3 shows that s1ZipA (A) and s2ZipA (B) remained stable attached to the bilayer after rinsing (vertical arrow) providing a flat baseline for subsequent buffer exchanges with different ionic strength.

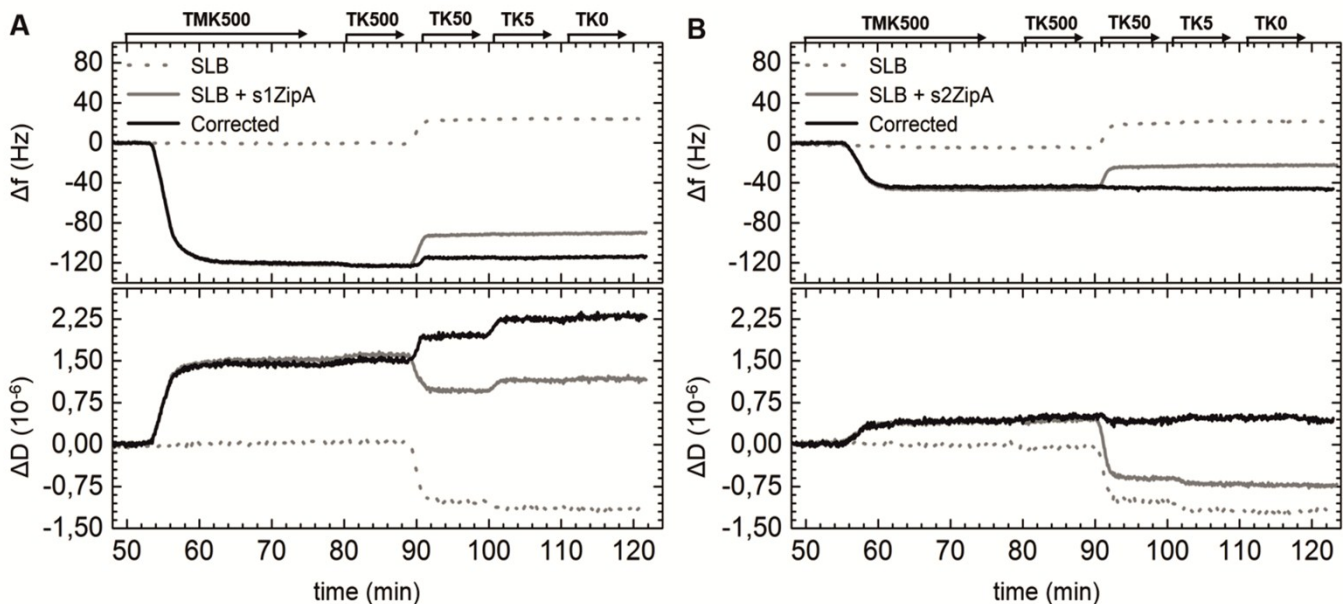
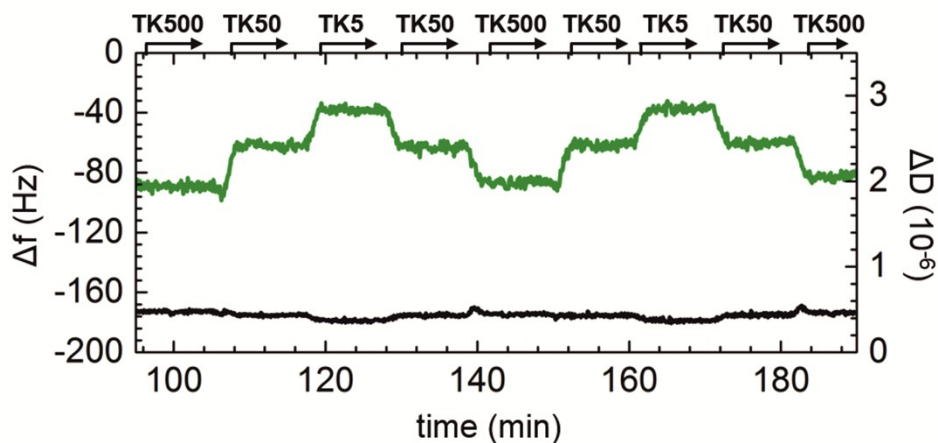


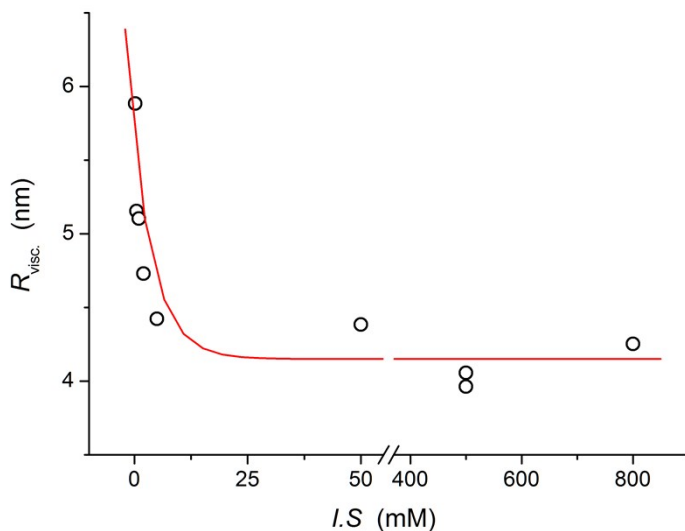
Figure S4. Baseline correction accounting for frequency and dissipation changes due to variation in buffer density and viscosity

Figure S4 shows frequency and energy dissipation changes in absence (dashed) and presence (light gray) of soluble constructs s1ZipA (A) and s2ZipA (B), registered simultaneously in independent fluid chambers for base line correction in real time. Contribution to the acoustic response due to the presence of proteins anchored to SLBs is then extracted by direct subtraction (bold).



**Figure S5.** Reversibility of acoustic response of s1ZipA upon buffer exchange with different salt content

At any specific surface coverage, after appropriate baseline subtraction, energy dissipation  $\Delta D$  (green) signals exhibit a step-like, fully reversible behavior upon salt content exchange (500/50/5 mM KCl). As can be seen in Fig. S5, there is almost zero frequency change  $\Delta f$  following the exchange of buffer as expected; the amount of protein remains fixed on the surface while only its shape changes – this shape change is reflected on  $\Delta D$  changes. The adsorption step of His-tagged s1ZipA to SLB containing NTA-DGS chelating lipids leading to a protein surface coverage of  $\approx -173$  Hz was omitted for clarity.



**Figure S6.** The viscosity radius dependence of s1ZipA on ionic strength content

The hydrodynamic radius  $R_h$ , calculated directly from the  $[\eta]$  experimental data and Eq. S1, is shown in Fig. S6. According to this graph, an apparent plateau value  $R_h \approx 4.1 \pm 0.1$  nm is measured at infinite ionic strength.

## References

1. R. Ahijado-Guzman, J. Prasad, C. Rosman, A. Henkel, L. Tome, D. Schneider, G. Rivas and C. Sonnichsen, *Nano Lett.*, 2014, **14**, 5528-5532.
2. S. E. Harding, *Prog. Biophys. Mol. Biol.*, 1997, **68**, 207-262.
3. M. L. Mansfield and J. F. Douglas, *J. Chem. Phys.*, 2013, **139**, 044901.
4. F. J. Moy, E. Glasfeld, L. Mosyak and R. Powers, *Biochemistry*, 2000, **39**, 9146-9156.
5. N. J. Cho, C. W. Frank, B. Kasemo and F. Hook, *Nat. Protoc.*, 2010, **5**, 1096-1106.